Cav1.1 controls frequency-dependent events regulating adult skeletal muscle plasticity

Gonzalo Jorquera[1], Francisco Altamirano[1], Ariel Contreras-Ferrat[1], Gonzalo Almarza[1], Sonja Buvinic[1,2], Vincent Jacquemond[3], Enrique Jaimovich[1] and Mariana Casas[1,4,*]

[1]Centro de Estudios Moleculares de la Célula, ICBM, Facultad de Medicina, Universidad de Chile, Independencia 1027-8380453, Santiago, Chile
[2]Departamento de Ciencias Básicas y Comunitarias, Facultad de Odontología, Universidad de Chile, Sergio Livingstone Pohlhammer 943-8380492, Santiago, Chile
[3]CNRS, UMR 5534, Université Lyon 1, Centre de Génétique et de Physiologie Moléculaire et Cellulaire, Bâtiment Raphaël Dubois, 43 Boulevard du 11 novembre 1918, 69622 Villeurbanne, France
[4]Programa de Fisiología y Biofísica, Instituto de Ciencias Biomédicas, Facultad de Medicina, Universidad de Chile, Independencia 1027-8380453, Santiago, Chile
*Author for correspondence (mcasas@med.uchile.cl)

Accepted 11 December 2012
Journal of Cell Science 126, 1189–1198

doi: 10.1242/jcs.116855

Summary

An important pending question in neuromuscular biology is how skeletal muscle cells decipher the stimulation pattern coming from motoneurons to define their phenotype as slow or fast twitch muscle fibers. We have previously shown that voltage-gated L-type calcium channel (Cav1.1) acts as a voltage sensor for activation of inositol (1,4,5)-trisphosphate [Ins(1,4,5)P_3]-dependent Ca^{2+} signals that regulates gene expression. ATP released by muscle cells after electrical stimulation through pannexin-1 channels plays a key role in this process. We show now that stimulation frequency determines both ATP release and Ins(1,4,5)P_3 production in adult skeletal muscle and that Cav1.1 and pannexin-1 colocalize in the transverse tubules. Both ATP release and increased Ins(1,4,5)P_3 was seen in flexor digitorum brevis fibers stimulated with 270 pulses at 20 Hz, but not at 90 Hz. 20 Hz stimulation induced transcriptional changes related to fast-to-slow muscle fiber phenotype transition that required ATP release. Addition of 30 μM ATP to fibers induced the same transcriptional changes observed after 20 Hz stimulation. Myotubes lacking the Cav1.1-α1 subunit released almost no ATP after electrical stimulation, showing that Cav1.1 has a central role in this process. In adult muscle fibers, ATP release and the transcriptional changes produced by 20 Hz stimulation were blocked by both the Cav1.1 antagonist nifedipine (25 μM) and by the Cav1.1 agonist (-)S-BayK 8644 (10 μM). We propose a new role for Cav1.1, independent of its calcium channel activity, in the activation of signaling pathways allowing muscle fibers to decipher the frequency of electrical stimulation and to activate specific transcriptional programs that define their phenotype.

Key words: Excitation–transcription coupling, Gene expression, DHPR, Frequency decoding, Extracellular ATP, Muscle plasticity

Introduction

Excitable cells can evoke a large number of physiological events in response to plasma membrane depolarization. For instance, a single action potential may induce massive intracellular Ca^{2+} release in muscle cells that produces muscle fiber contraction and may trigger neurotransmitter release in neurons. Additionally, most excitable cells, notably muscle cells and neurons, respond not only to single depolarization events, but also to complex patterns of depolarizing stimuli of varying durations and frequencies. Consequently, a train of action potentials at a defined frequency is no longer an all or none message, but a code that excitable cells decipher to activate different process that determine their behavior. For example, spike-bursting patterns appear important for information processing and memory acquisition in neurons (Harris et al., 2001; Xu et al., 2012). In skeletal muscle fibers, different stimulation patterns activate diverse signaling pathways that ultimately define their phenotype (Schiaffino et al., 2007). Adult skeletal muscle contains different types of muscle fibers, which vary in both the speed of contraction and force generation and in their resistance to fatigue. Accordingly, muscle fibers can be classified generally as fatigue resistant slow-twitch fibers or as fast-twitch fibers that are either fatigue resistant or fatigable. Fatigue resistant slow-twitch fibers rely on their ATP supply mainly via oxidative metabolism that confers them their fatigue resistance, whereas fast-twitch fibers rely mainly on glycolytic metabolism as a source of ATP. These different fiber phenotypes can change in response to changes in activity demands, leading to a gradual switch from one fiber type to another. This process is known as muscle plasticity.

Nerve activity plays a major role in the specification and maintenance of skeletal muscle fibers phenotype, which depends on both myoblast lineage and motoneuron innervation (Gunning and Hardeman, 1991; DiMario and Stockdale, 1997; Kalhovde et al., 2005). Importantly, external electrostimulation with different firing patterns corresponding to different motoneuron subclasses allows the establishment of specific transcriptional programs that control fiber-type identity and growth and can provoke fiber phenotype transition by inducing the expression of specific myosin heavy chains and other contractile proteins as well as metabolic enzymes (Pette and Vrbová, 1985; Murgia et al., 2000; Serrano et al., 2001; Kubis et al., 2002). In particular,

Troponin I is a protein of the contractile machinery which possesses two isoforms that are differentially expressed in distinct muscle fibers types (Banerjee-Basu and Buonanno, 1993) and whose regulation is under nerve activity control (Calvo et al., 1996; Rana et al., 2009). Expression of the slow Troponin I (TnIs) isoform is restricted to slow-twitch fibers while the fast isoform (TnIf) is restricted to fast-twitch fibers; both isoforms are downregulated in denervated muscles. External electrical stimulation of the denervated muscle with a slow pattern (10 Hz) induces a specific upregulation of the TnIs gene, while stimulation with a fast pattern (100 Hz) upregulates TnIf (Calvo et al., 1996). This feature makes TnI isoforms good markers of the transcriptional changes that occur in fibers during the muscle plasticity process.

In spite of the physiological importance of the ability of muscle cells to decipher different electrical stimulation patterns, the molecular mechanisms involved in muscle plasticity remain largely unknown. Changes in intracellular Ca^{2+} concentration have been proposed extensively to mediate cellular responses to electrical stimulation. It was proposed that a train of action potentials with a defined frequency induces a characteristic train of Ca^{2+} release events that, in turn, differentially activate particular Ca^{2+}-dependent signaling pathways that determine the expression of genes responsible for the slow or fast muscle phenotype (Chin, 2004). These signaling pathways include the calcineurin–NFAT, Ca^{2+}/calmodulin-dependent kinases II and IV (CaMKII and CaMKIV) and protein kinase C (PKC) pathways (Chin et al., 1998; Liu et al., 2001; Serrano et al., 2001; Wu et al., 2002).

Muscle cells present a complex pattern of Ca^{2+} transients under depolarization that are related to both excitation-contraction (E–C) coupling and excitation-transcription (E–T) signaling. In adult muscle cells, depolarization of the transverse-tubule (T-tubule) membrane induces a conformational change in Cav1.1 when transmitted to the ryanodine receptor (RyR1), causes channel opening and Ca^{2+} release from the sarcoplasmic reticulum (SR) to induce fiber contraction. In addition to this canonical signal, sustained depolarization stimulates inositol 1,4,5-trisphosphate receptor [Ins(1,4,5)P_3R]-mediated Ca^{2+} release that generates slow, long-lasting Ca^{2+} transients (Jaimovich et al., 2000). These slow transients, not related to muscle contraction, regulate several transcription-related events following membrane depolarization (Carrasco et al., 2003; Juretić et al., 2007). The signaling pathway activated by depolarization of muscle cells and triggered by Cav1.1 includes the sequential activation of G protein, phosphatidylinositide 3-kinase (PI3K) and phospholipase C (PLC) to produce inositol (1,4,5)-trisphosphate [Ins(1,4,5)P_3] that causes Ca^{2+} release via Ins(1,4,5)P_3R present in the SR membrane as well as in the nucleus (Cárdenas et al., 2005; Eltit et al., 2006). Electrical stimulation of cultured myotubes also promotes ATP release, likely through pannexin-1 (Panx1) channels. This ATP released is a key step in the onset of slow Ins(1,4,5)P_3-dependent Ca^{2+} signals, acting through P2X and P2Y receptors to modulate the process of E–T coupling (Buvinic et al., 2009).

In adult muscle, Cav1.1 also mediates the activation of slow Ins(1,4,5)P_3-dependent Ca^{2+} signals; their amplitude depends on both the duration and frequency of stimulation, with a maximum at 10–20 Hz. At this stimulation frequency, an increase of TnIs and a decrease in TnIf mRNA levels take place (Casas et al., 2010), a characteristic feature of fast-to-slow fiber phenotype transition.

In the present work, we describe that both Ins(1,4,5)P_3 production and ATP release are frequency-dependent events in adult skeletal muscle fibers, controlled by Cav1.1 acting as both a voltage sensor and a frequency decoder. Furthermore, Cav1.1 colocalizes with Panx1 channels in the T-tubule, suggesting the possible interaction between these two molecules to trigger ATP release. This is a major advance in the comprehension of the molecular events underlying activation of different signaling pathways by different patterns of stimulation that are the basis of skeletal muscle plasticity.

Results

Ins(1,4,5)P_3 production and ATP release are frequency-dependent events in adult skeletal muscle fibers

We investigated if molecular events upstream of Ins(1,4,5)P_3-dependent Ca^{2+} signals were sensitive to stimulation frequency. Adult flexor digitorum brevis (FDB) muscle fibers were stimulated with 270 pulses, 0.3 ms each, at different frequencies, measuring the generation of Ins(1,4,5)P_3 and ATP release at different times after stimulation. Fibers stimulated at 20 Hz displayed two peaks of Ins(1,4,5)P_3 production, at 15 s and 5 min after stimulation, whereas fibers stimulated at 90 Hz did not increase their Ins(1,4,5)P_3 levels (Fig. 1A). After 20 Hz stimulation Ins(1,4,5)P_3 increased from 0.021±0.001 pg/mg protein to 0.048±0.014 pg/mg protein in the first peak and to 0.054±0.013 pg/mg protein in the second peak. ATP release has a bell shape curve dependency on frequency of stimulation, showing a maximum at 20 Hz and almost no ATP release at frequencies higher than 60 Hz (Fig. 1B). Similarly to Ins(1,4,5)P_3 production, fibers stimulated at 20 Hz exhibited an increase in extracellular ATP levels with two peaks, reaching levels of almost 15-fold over non-stimulated conditions (typical trace in Fig. 1C, mean of maximum release in Fig. 1D). For most cells, the first peak occurs between 15 and 30 s after stimulation and the second between 3 and 5 min later (supplementary material Fig. S1). Average basal ATP levels were 11.1±3.5 pmol ATP/µg RNA, increasing to 166.1±67.5 and 165.2±75.5 pmol ATP/µg RNA for the first and second peak respectively, after stimulation. Interestingly, extracellular ATP levels did not increase when fibers were stimulated at 90 Hz (Fig. 1B–D). The increase in extracellular ATP levels observed at 20 Hz decreased significantly in cells treated with 5 µM carbenoxolone (CBX). At this concentration, carbenoxolone selectively blocks pannexin channels (Huang et al., 2007), 5–20 fold higher concentration is required for connexin hemichannel blockade (Bruzzone et al., 2005), suggesting that pannexin channels mediate ATP release (Fig. 1E,F).

Ins(1,4,5)P_3-dependent Ca^{2+} signals participate in plasticity-related transcriptional changes that depend on ATP release

As previously shown, adult FDB muscle fibers stimulated at 20 Hz exhibit an increase in TnIs and a decrease in TnIf mRNA levels 4 h after the stimulus, a signature of fast-to-slow muscle fiber phenotype transition (Casas et al., 2010). These transcriptional changes required functional Ins(1,4,5)P_3R because they did not occur in fibers pre-incubated during 30 min with 5 µM XestospongiB (XB), an Ins(1,4,5)P_3R inhibitor (Fig. 2A). Stimulation at 90 Hz produced the opposite effects: a decrease in TnIs and an increase in TnIf mRNA levels. These changes,

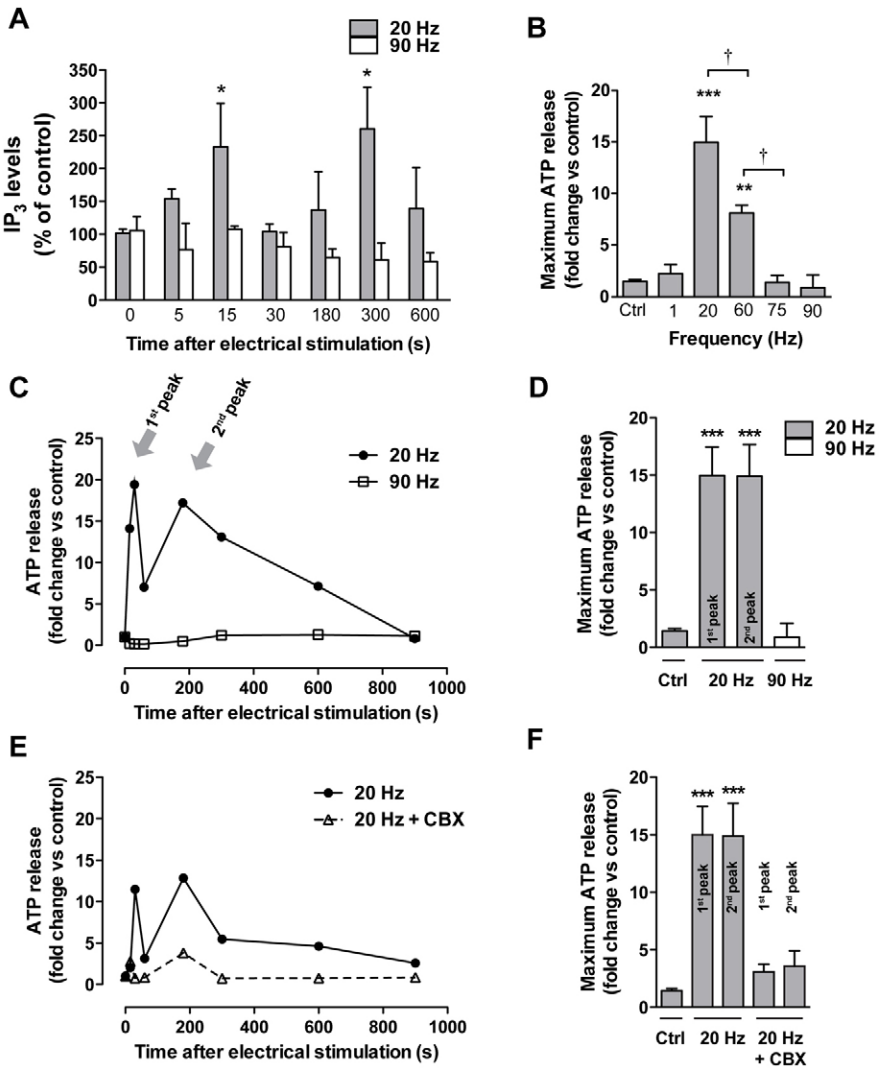

Fig. 1. Ins(1,4,5)P_3 production and ATP release depend on stimulation frequency. Adult FDB muscle fibers were stimulated with 270 pulses, 0.3 ms each, at different frequencies and Ins(1,4,5)P_3 (IP_3) production and ATP release were measured at different times after stimulation. (**A**) Fibers stimulated at 20 Hz displayed two peaks of Ins(1,4,5)P_3 production. Fibers stimulated at 90 Hz did not increase their Ins(1,4,5)P_3 levels (n=3). (**B**) ATP release depends on the frequency of stimulation; maximum values for different frequencies tested are reported. (**C**) In fibers stimulated at 20 Hz we observed two peaks of ATP release, while in fibers stimulated at 90 Hz there was practically no ATP release. (**D**) Quantification of maximum release at 20 Hz and 90 Hz (n=6). (**E**,**F**) ATP release was measured in the presence or absence of the panx1 inhibitor carbenoxolone (CBX, 5 µM; n=4). (E) Examples of the release of ATP with (open triangles) and without CBX (filled circles) and (F) quantification of maximum ATP release. ***P<0.001; **P<0.01; */$^{\dagger}P$<0.05.

however, were independent of Ins(1,4,5)P_3R because pre-incubation with XB had no effect (Fig. 2A). Changes observed in TnI mRNA levels were controlled at the transcriptional level because they were suppressed by pre-incubation of muscle fibers with 1.5 µM Actinomycin D, a transcription blocker (supplementary material Fig. S2A). We examined if ATP released after 20 Hz stimulation plays a role in the transcriptional changes in TnI genes described above. ATP release blockage with Panx1 inhibitor CBX suppressed the changes in TnIs and TnIf mRNA levels produced by stimulation at 20 Hz (Fig. 2A). Similarly, we found no increment in TnIs mRNA levels after stimulation at 20 Hz in fibers pre-incubated for 30 min with 2 U/ml apyrase, a nucleotidase that metabolizes extracellular ATP to AMP (Fig. 2B). Moreover, we found that addition of 30 µM ATP induced an increase in intracellular Ins(1,4,5)P_3 levels, which peaked 60 s after ATP addition (Fig. 2C), going from 0.015±0.002 pg/mg protein to 0.026±0.003 pg/mg protein. In agreement, addition of 30 µM ATP induced the same transcriptional changes in TnI genes produced by stimulation at 20 Hz (Fig. 2D). We tested other ATP concentrations, ranging from 10 to 100 µM (supplementary material Fig. S2B); we chose 30 µM because at this concentration the transcriptional changes observed were more prominent.

Cav1.1 controls the first step of frequency decoding acting as a voltage sensor for Ins(1,4,5)P_3 and ATP-dependent transcriptional changes observed at 20 Hz

We measured extracellular ATP levels in dysgenic (*mdg*) myotubes that do not express the α_1s subunit of Cav1.1 (the subunit bearing the voltage sensor), after stimulation with 100 pulses at 20 Hz. In these cells, electrical stimulation did not evoke any Ca^{2+} transient due to the absence of the Cav1.1 α_1s subunit (supplementary material Fig. S3). The typical traces of ATP release in Fig. 3A show practically no response after electrical stimulation of dysgenic myotubes as compared to myotubes from wild-type mice. In wild-type cells ATP increased from 6.05±0.71 to 63.11±13.76 and 60.23±5.44 pmol/µg RNA for the first and second peak respectively, while in *mdg* myotubes ATP release went from 28±3.79 pmol/µg RNA to 55.82±8.61 and 62.83±7.07 pmol/µg RNA for the first and second peak (see Fig. 3B for fold changes).

To evaluate the corresponding role of Cav1.1 in adult muscle fibers, FDB fibers were stimulated at 20 Hz in the presence of nifedipine to inhibit Cav1.1 function. We found that 25 µM nifedipine produced a marked decrease in ATP release relative to the controls measured at different times after stimulation, as

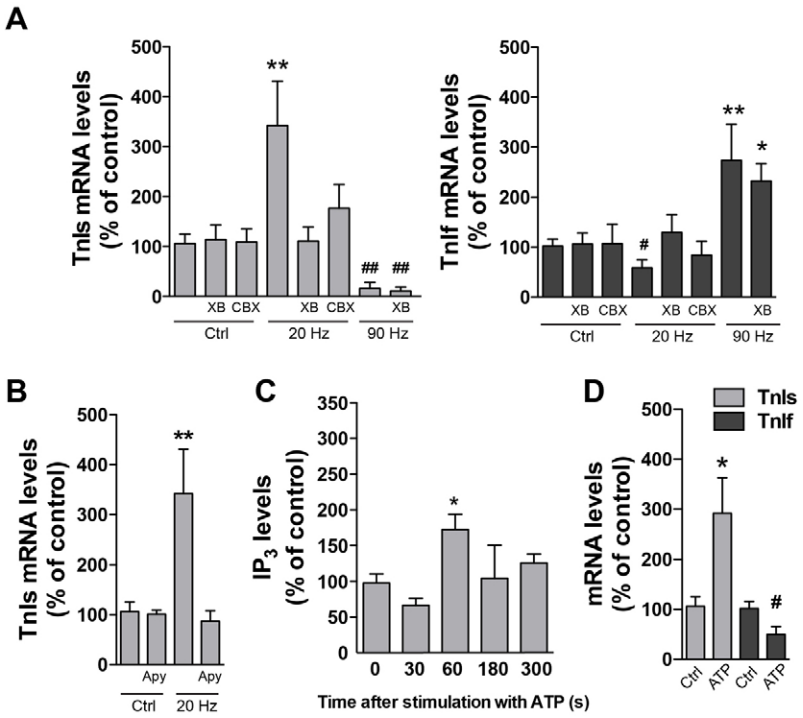

Fig. 2. Fast-to-slow phenotype-related transcriptional changes in adult muscle fibers are dependent on Ins(1,4,5)P_3R and ATP release. mRNA levels of TnIs and TnIf were determined 4 h after the stimulation of adult FDB muscle fibers at 20 Hz or 90 Hz. (**A**) 20 Hz stimulation induced an increase in TnIs and a decrease in TnIf mRNA levels. These transcriptional changes were abolished by pre-incubation of fibers for 30 min with 5 µM XestosponginB (XB), an Ins(1,4,5)P_3R inhibitor (n=4). At 90 Hz, a decrease in TnIs and an increase in TnIf mRNA levels were observed. These changes were not blocked by XB (n=4). (**B**) The increase in TnIs mRNA levels observed at 20 Hz was completely lost by pre-incubation of fibers with 2 U/ml apyrase (Apy) for 30 min (n=3). (**C**,**D**) Addition of 30 µM external ATP to fibers induced an increase in intracellular Ins(1,4,5)P_3 levels (C) as well as the same transcriptional changes of TnI genes (D) as observed after electrical stimulation at 20 Hz (n=3). **/$^{\#\#}P$<0.01; */$^{\#}P$<0.05.

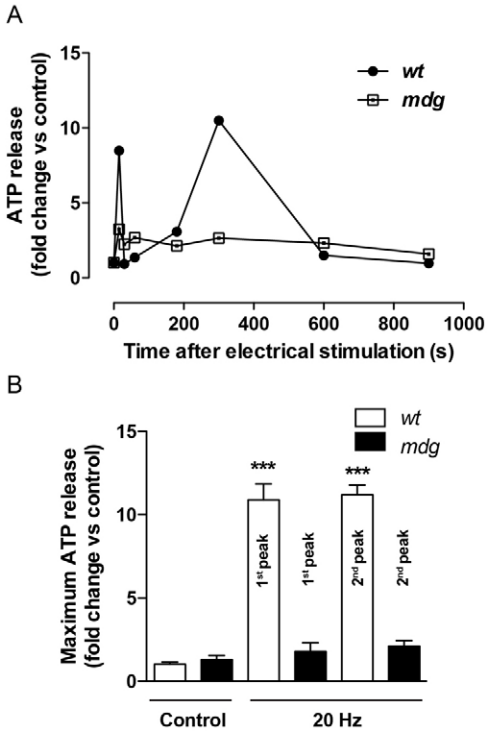

Fig. 3. Cav1.1 is necessary for ATP release after electrical stimulation in primary myotubes. (**A**,**B**) Primary myotubes from wild-type (wt) mice or dysgenic (*mdg*) mice, lacking the α_1s subunit of the Cav1.1 channel were stimulated at 20 Hz as in Fig. 1. (A) ATP release was measured at different times after stimulation. (**B**) Quantification of the first and second peak of release in both cell types. ATP release was significantly inhibited in *mdg* myotubes compared with wild-type cells (n=3). ***P<0.01.

shown in Fig. 4A (quantification of peaks is shown in Fig. 4B). Moreover, we found that the increase in TnIs and decrease in TnIf mRNA levels observed in controls did not occur in fibers treated with nifedipine (Fig. 4C), suggesting a blockade of the whole signaling process.

We have previously shown that post-tetanic Ins(1,4,5)P_3-dependent Ca^{2+} signals in adult skeletal muscle fibers are independent from Ca^{2+} entry (Casas et al., 2010). Consequently, we hypothesized that the involvement of Cav1.1 in E–T coupling corresponds to a different and Ca^{2+} channel-independent function of this protein. To test this hypothesis, we stimulated at 20 Hz muscle fibers previously incubated for 20 min with 10 µM (-)S-BayK 8644 (BayK), another dihydropyridine that behaves as a Cav1.1 agonist, and measured ATP release and mRNA levels of both TnI isoforms. We found that this agonist inhibited ATP release (Fig. 4A,B) and prevented the changes in TnIs and TnIf mRNA levels produced by 20 Hz electrical stimulation (Fig. 4C). Interestingly, these two drugs had opposite effects on Ca^{2+} currents through Cav1.1 in adult fibers. Nifedipine produced an almost complete inhibition of the Ca^{2+} current whereas BayK enhanced the peak current amplitude and shifted the voltage-dependence towards more negative values (Fig. 5).

Cav1.1 and Pannexin-1 channels appear to be part of the same signaling complex

In order to understand the mechanism allowing Cav1.1 to control ATP release via Panx1 channels, we looked for a possible protein–protein interaction between these two molecules. We performed an *in situ* proximity ligation assay (PLA) with probes for Panx1 and Cav1.1 α1s subunit in non-stimulated fibers (Fig. 6) and 1 min after 20 Hz or 90 Hz stimulation (supplementary material Fig. S4A). We observed that immunofluorescence against Cav1.1 α1s subunit shows a clear

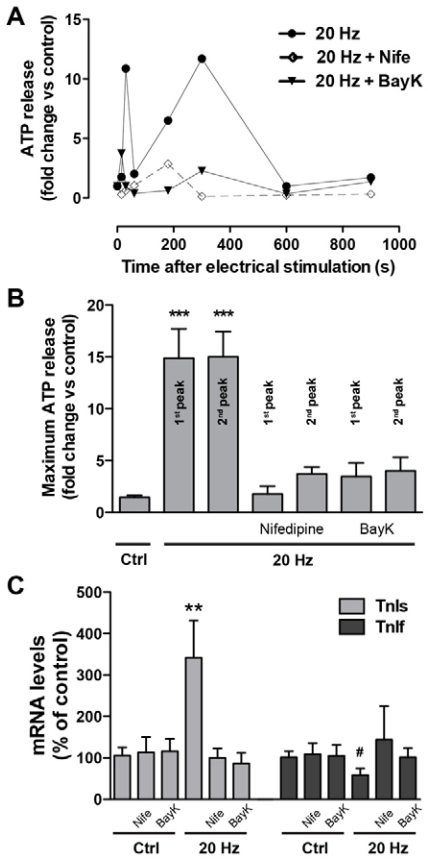

Fig. 4. Cav1.1 controls the first step of frequency decoding. Adult FDB muscle fibers were stimulated at 20 Hz as in Fig. 1. (**A**) ATP release was measured at different times after stimulation in untreated fibers (filled circles) and in fibers pre-incubated for 20 min with 25 µM of the channel antagonist Nifedipine (open diamonds) or with 10 µM of the channel agonist (-)S-BayK 8644 (filled triangles) ($n=3$). (**B**) Quantification of the first and second peak of release with or without each drug. (**C**) In fibers pre-incubated for 20 min with either drug, the typical increase in TnIs and decrease in TnIf mRNA levels were suppressed ($n=3$). ***$P<0.001$; **$P<0.01$; $^{\#}P<0.05$.

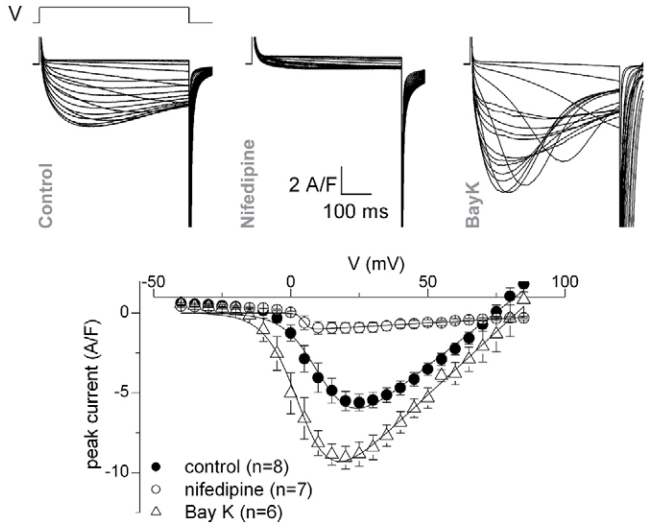

Fig. 5. Opposite effects of Nifedipine and (-)S-BayK 8644 on depolarization-evoked Ca^{2+} current through Cav1.1 in adult muscle. Ca^{2+} currents were measured in FDB muscle from adult mice under voltage clamp conditions. Top panel: representative Ca^{2+} current traces recorded in a control fiber (left), in a fiber treated with 25 µM nifedipine (middle) and one treated with 10 µM (-)S-BayK 8644 (right). Records were obtained in response to 0.5 s-long depolarizing steps from −80 mV to values ranging between −20 and +65 mV. Bottom panel: mean voltage dependence of the peak Ca^{2+} current measured in control conditions (filled circles), in the presence of nifedipine (open circles) or in the presence of (-)S-BayK 8644 (triangles).

double-striated pattern as expected for a protein located in the transverse tubules (Fig. 6A, bottom panels). Panx1 immunostaining shows a preponderant fluorescence near the surface and also a striated signal that runs at both sides of the z-line (labeled with anti-α-actinin antibody), suggesting a T-tubule localization for this protein as well (Fig. 6A, upper panels). This signal appears weaker towards the center of the fiber (Fig. 6C, right). *In situ* PLA probes for Panx1 and Cav1.1 α1s show a well-defined protein–protein interaction in non-stimulated (Fig. 6B,C) as well as in 20 Hz stimulated muscle fibers (supplementary material Fig. S4A), with no apparent differences. PLA probes in fibers after 90 Hz stimulation gave variable results, the mean being smaller than those after 20 Hz or basal conditions (supplementary material Fig. S4A). Indirect immunofluorescence against RyR1 was used to define fiber structure in this assay (Fig. 6B). PLA labeling appears to be concentrated near the surface (up to a depth of 4–5 µm), as can be seen in the z-projection for the whole fiber and in the correspondent fluoresce profiles of the center of the fiber (dashed line; Fig. 6B,C). As control we explored the PLA probes using antibodies against α-actinin, a structural protein that marks Z-disk and SERCA1, sarco-endoplasmic reticulum Ca^{2+} ATPase, that is expressed in non junctional sarcoplasmic reticulum. Even when the immunofluorescence for these two proteins gave a clear and strong labeling (α-actinin in Fig. 6A, upper right panel; supplementary material Fig. S5, SERCA1), there was a poor signal for PLA when using α-actinin/SERCA1 probes (Fig. 6D), as expected for two proteins that do not interact. After α-actinin/SERCA1 PLA was performed, indirect immunofluorescence against RyR1 was used to define fibers structure (Fig. 6D, lower panel).

We also tested the Panx1/Cav1.1 interaction by co-immunoprecipitation of these proteins from triad's enriched fractions of skeletal muscle. Characterization of this fraction is shown in Fig. 6E. We observed that Cav1.1 co-immunoprecipitated with Panx1 (Fig. 6F), but not with dysferlin, another protein present in triads extracts and used here as a negative control for co-immunoprecipitation essay (supplementary material Fig. S4B). These results suggest a direct protein–protein interaction between Cav1.1 and Panx1 channels, allowing us to hypothesize that control exerted by Cav1.1 over ATP release via Panx1 channels may be through a conformational change of this molecule somehow transmitted to Panx1.

Discussion

In adult skeletal muscle, stimulation frequency regulates activation of specific transcriptional programs that help to define and adapt the muscle fiber phenotype. Ever since the role of nerve stimulation in muscle plasticity process was demonstrated (Buller et al., 1960; Pette and Vrbová, 1985; Schiaffino et al., 1999), a series of hypotheses have been proposed to explain how nerve stimulation modifies the transcription of specific genes. As in response to each action

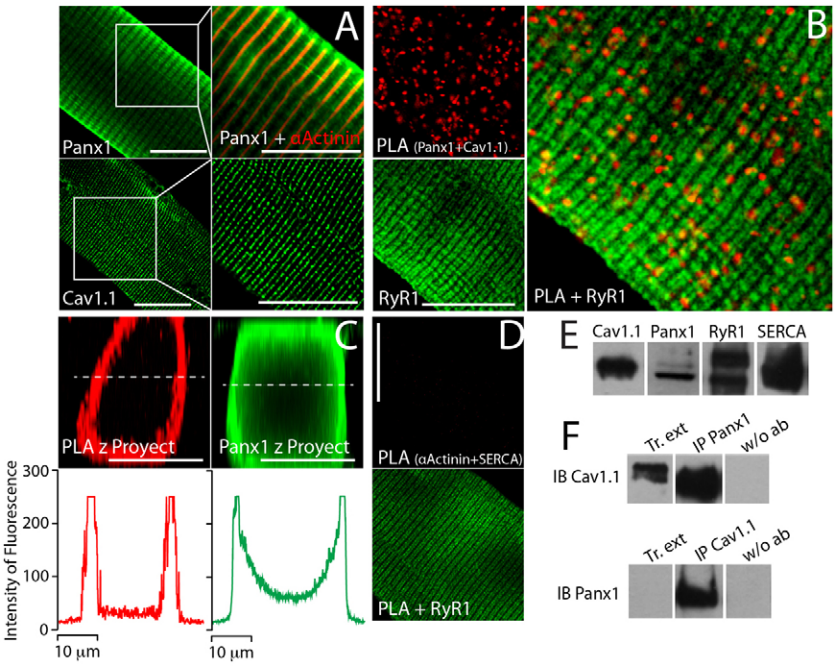

Fig. 6. Cav1.1 and Pannexin-1 channels interact in the T-tubule of adult muscle fibers. (**A**) Immunostaining for Panx1 (upper panels) and Cav1.1 α1s subunit (lower panels) in 1 μm confocal slices of adult muscle fibers. Panx1 is present in the sarcolemma and also in a striated pattern that runs on both sides of the z-line, detected by α-actinin staining. Anti-Cav1.1 α1s subunit antibody shows the clear striated pattern of a T-tubule protein. (**B**) *In situ* proximity ligation assay (PLA) probes for Panx1 and Cav1.1 α1s show a well-defined protein–protein interaction; RyR1 staining is shown to define fiber structure (a merged image is shown in the right panel). The image shown is of a slice from near the surface of the fiber. (**C**) z-projection reconstructions for the whole fiber, confirming the PLA labeling of the interaction between Panx1 and Cav1.1 in a region near the surface (left panels). Similarly Panx1 immunostaining shows a preponderant peripheral location (right panels). Graphs at the bottom show the fluorescence profile at the position of the dashed line in the upper panels. (**D**) As negative control, *in situ* PLA was performed with α-actinin and SERCA probes (co-stained with RyR1 in lower panel) and shows no labeling. Scale bars: 20 μm. (**E**) In triads fractions derived from BalbC mouse muscles, we observed the presence of Cav1.1, Panx1, RyR1 and SERCA. (**F**) In the fractions in E, Cav1.1 co-immunoprecipitated with Panx1 (upper panel) as Panx1 co-immunoprecipitated with Cav1.1 (lower panel). In the latter, Panx1 is not visible in triads extract (Tr. ext, first lane) because exposure time was optimized to visualize the immunoprecipitate. A representative image from three different experiments is presented.

potential there is a rapid increase in intracellular Ca^{2+} via RyR1, stimulation at different frequencies could be expected to induce different patterns of intracellular Ca^{2+} signals to differentially activate Ca^{2+}-dependent signaling pathways leading to activation of specific transcription programs proper of one fiber type or another (Hughes, 1998; Spangenburg and Booth, 2003). In this regard, it was described that Ca^{2+} signal amplitudes associated to each stimulation train was larger at higher than at lower frequencies (Chin, 2004). Fiber type differences in expression of Ca^{2+}-related proteins such as parvalbumin, SERCA, Cav1.1 and RyR1 also contributed to sustain this hypothesis (Lamb, 1992; Delbono and Meissner, 1996; Chin et al., 2003). Nevertheless, the mechanism underlying differential activation of signaling pathways at the plasma membrane remains elusive. In the present work, we evidence a molecular sensing system in adult skeletal muscle fibers that decodes stimulation frequency at the plasma (T-tubule) membrane, linked to Cav1.1 activation, pannexin-mediated ATP release and Ins(1,4,5)P_3 production.

We have previously described that membrane depolarization of skeletal myotubes evokes Ins(1,4,5)P_3-dependent Ca^{2+} signals triggered by Cav1.1 and related to E–T coupling. In these cells, ATP released through Panx1 channels after electrical stimulation plays an important role in this process (Buvinic et al., 2009). In electrically stimulated adult muscle fibers, Ins(1,4,5)P_3-evoked Ca^{2+} signals mediate the frequency-dependent activation of slow-phenotype muscle fiber genes (TnIs) and repression of fast-phenotype fibers genes (TnIf) (Casas et al., 2010). In a recent publication (Blaauw et al., 2012), lack of calcium signals in response to Ins(1,4,5)P_3 uncaging in adult muscle fibers was reported; there are several reasons why such signals may be hard to record, including some dependence of Ins(1,4,5)P_3-induced Ca^{2+} release on membrane potential and/or intracellular Ca^{2+} concentration (Rojas and Jaimovich, 1990) or even mitochondria dumping of the calcium transient (Eisner et al., 2010). The fact that such transients can be evidenced after tetanic stimulation (Casas et al., 2010) and that Ins(1,4,5)P_3R inhibition blocks expression of particular genes, suggests that the precise location, magnitude and regulation of this signaling system should be a matter of further studies. Still, evidence from other groups also shows the presence of functional Ins(1,4,5)P_3R in adult muscle fibers (Volpe et al., 1985) and Ins(1,4,5)P_3 production after muscle stimulation (Vergara et al., 1985; Mayr and Thieleczek, 1991).

Now, we show that ATP release in adult muscle fibers after electrical stimulation is frequency dependent, occurring in fibers stimulated at 20 Hz but not at 90 Hz (Fig. 7). We also show that ATP release plays a key role in transcription of the slow-type TnI gene induced by 20 Hz stimulation, because fibers treated with apyrase to hydrolyze ATP, or CBX to inhibit ATP release by inhibition of Panx1 channels, did not exhibit the changes in mRNA levels produced at this stimulation frequency. Moreover,

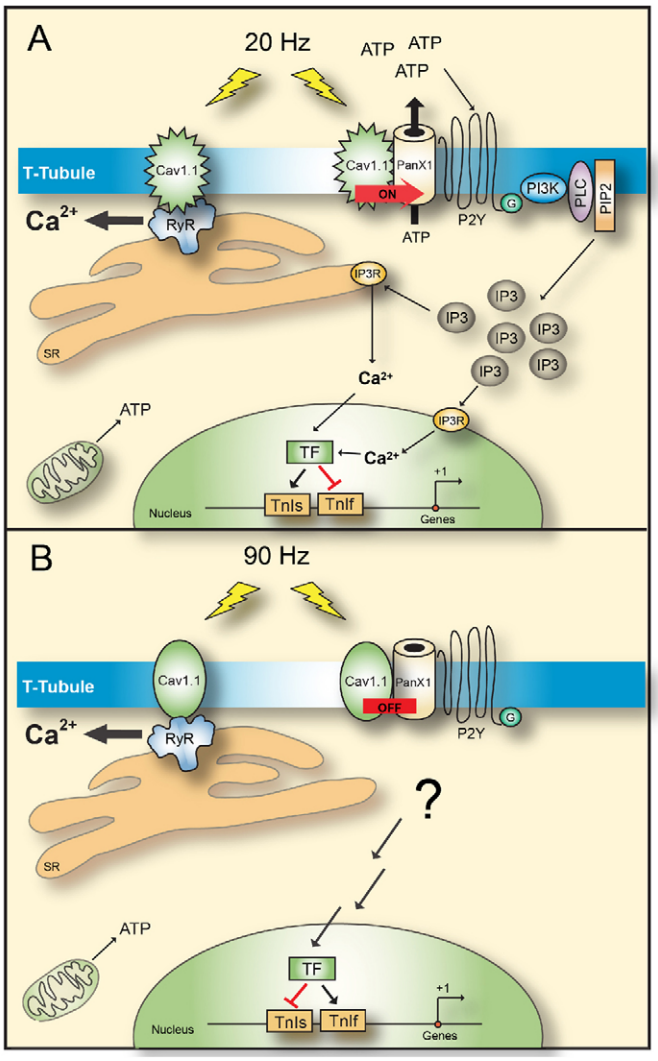

Fig. 7. Working model. (**A**) 20 Hz electrical stimulation in adult FDB fibers activates Cav1.1 with each depolarizing event. This activation in turn, induces a fast Ca^{2+} release through RyR1 that causes muscle fiber contraction. We propose that at this frequency, there is an activation of another function of Cav1.1 related to Panx1 activation causing ATP release. These events will trigger in turn a signaling cascade where, through activation of P2Y receptors, PI3K and PLC, the consequent Ins(1,4,5)P_3 (IP_3) production at the plasma membrane will induce a Ca^{2+} signal via Ins(1,4,5)P_3R responsible for activation of genes related to a fast-to-slow muscle fiber transition. (**B**) At 90 Hz stimulation, each pulse will also activate Ca^{2+} release via RyR1, producing fiber contraction, nevertheless, at this frequency, we hypothesize that triggering of the Cav1.1 function related to Panx1 activation to induce ATP release is not reached, so at this frequency, this function remains switched off. In this case, the signaling cascade leading to Ins(1,4,5)P_3 production and Ca^{2+} release via Ins(1,4,5)P_3R does not take place. However, other signaling pathways are activated at this frequency, inducing transcriptional changes related to slow-to-fast muscle fiber transition.

extracellular addition of 30 µM ATP induced the same transcriptional changes in TnI genes as electrical stimulation at 20 Hz. The fact that external ATP increased Ins(1,4,5)P_3 levels suggests that these transcriptional events occur in response to the same signaling pathways elicited by 20 Hz electrical stimulation or by external ATP addition.

In the last few years, ATP has been increasingly considered as an extracellular messenger for autocrine and paracrine signaling (Corriden and Insel, 2010). Several studies have recently demonstrated that ATP can be released by pannexin channels in a variety of cell types that include myotubes (D'Hondt et al., 2011). The widespread distribution of Panx1 has been confirmed in several tissues, with the highest levels in skeletal muscle (Baranova et al., 2004). In this work we show that Panx1 channels are located at the sarcolemma and at the T-tubules in skeletal muscle fibers.

We have shown that Cav1.1 forms part of the mechanism regulating ATP release after electrical stimulation of muscle cells. Thus, ATP release is practically absent after electrical stimulation of myotubes lacking the α1 subunit of this channel (impairing the assembly of the whole channel at the plasma membrane), while in adult muscle fibers the Cav1.1 blocker nifedipine abolished both ATP release and the transcriptional changes produced by 20 Hz stimulation. Interestingly, (-)S-BayK 8644 (BayK) also inhibited these two processes, albeit it had the opposite effect on Ca^{2+} current through the Cav1.1 channel than nifedipine. We have previously shown that Ins(1,4,5)P_3-dependent Ca^{2+} signals are independent from extracellular Ca^{2+} entry (Casas et al., 2010). The fact that nifedipine and BayK have the same inhibitory effects on ATP release and gene expression indicates that the Ca^{2+} current through Cav1.1 is not relevant to activate the E–T coupling process. More importantly, it suggests the existence of a Ca^{2+}-current-independent function of Cav1.1, related to activation of E–T coupling that is blocked by these two drugs. In fact, the voltage gated Ca^{2+} channel (driving an L-type current) function of Cav1.1 is also irrelevant for the voltage sensor function in E–C coupling activation. Hence, the roles of Cav1.1 as voltage sensor in E–C coupling and E–T signaling, both activated by membrane depolarization, are independent of the function of Cav1.1 as Ca^{2+}-current carrier. The molecular mechanisms behind these different functions are not still completely established, but several mutations in Cav1.1 differentially affect Ca^{2+} currents and E–C coupling, suggesting that different parts of the Cav1.1 molecule would be responsible for each function (Beam and Bannister, 2010). This could also be the case for the activation of the signaling cascade presented here. Another and not excluding possibility is that different states of the protein during activation, possibly reached with different kinetics, could be involved in E–T signaling. Several lines of evidence suggest complex transitions of Cav1.1 and multiple intermediate states of the protein during activation. In frog muscle fibers, there are different components of charge movement, with different voltage activation dependence and different kinetic parameters (Ríos and Pizarro, 1991). Even when charge movement is amenable to modeling by only one component, different fractions of this charge movement could be associated to E–C coupling and to Ca^{2+} current through the pore. For instance, nifedipine inhibits only a fraction of charge movement (nifedipine sensitive Q; Q_{ns}) (Lamb and Walsh, 1987). In this condition, fibers maintain E–C coupling, showing that Q_{ns} is not necessary for the onset of E–C coupling, while the Q_{in} (insensitive to nifedipine) is. In that work, the authors suggest that the difference in time course between the charge movement Q_{ns} and the appearance of the Ca^{2+} current through Cav1.1 is possibly due to the existence of an intermediary state (occurring after Q_{ns}), with an associated charge movement too slow to be recorded. Interestingly, in muscle fibers treated with BayK,

charge movements appear unaffected (Lamb and Walsh, 1987). It is also possible then, that both drugs inhibit a charge movement with slow kinetics that might be responsible for the activation of the signaling pathway described here after stimulation at 20 Hz. Along this line, there is clear indication from the tail currents observed in BayK treated fibers that Cav1.1 deactivation is slowed-down in the presence of this drug (Johnson et al., 1997). Therefore, one possible explanation for our BayK results is that a slowed Cav1.1 configuration precludes activation of the ATP release and Ins(1,4,5)P_3 production machinery induced by 20 Hz stimulation. Following this view, in control adult fibers, the channel will be unable to activate ATP release at high frequencies (as 90 Hz) because the Cav1.1 activation kinetics for this process would not be fast enough. The bell-shaped curve of ATP release at different frequencies also supports this hypothesis, showing that beyond 20 Hz, ATP release decrease with increasing the frequency of stimulation to be lost at a frequency between 60 and 75 Hz. Further experiments with Cav1.1 mutants and drugs affecting the channel behavior to evaluate their effect on the frequency-decoding process described here would also shed light on the possible mechanism of E–T coupling activation by Cav1.1.

Importantly, the mechanisms of frequency decoding by Cav1.1 could be important for other excitable cells. In neurons, it has been shown that intracellular Ca^{2+} increases depending on Cav1 occurs at 10 Hz stimulation but not at 100 Hz and this Ca^{2+} increase has an important role in CREB activation (Wheeler et al., 2012).

We have presented here evidence indicating that both Cav1.1 and Panx1 are located in a region of the T-tubule membrane and a close association between these two molecules was evidenced by the *in situ* PLA method, which gives positive labeling for proteins located at a distance of less than 40 nm. This suggests the possibility of a direct protein–protein interaction. Consistent with a stronger Panx1 labeling near the fiber surface, interaction with Cav1.1 appears also to be concentrated in a region of the T-tubules at 4 to 5 μm from the sarcolemma. Considering a precise conformational change of Cav1.1 which could be responsible for ATP release, this conformational change could be directly linked to Panx1 activation via a protein–protein interaction between these two molecules, probably at the T-tubules. The fact that PLA gives the same labeling in control and in fibers stimulated at 20 Hz suggest the presence of a pre-assembled signaling protein complex that may be activated by conformational changes of some of its components after stimulation, as has been already be proposed in other models (Galés et al., 2006; Halls and Cooper, 2010). The difference found after 90 Hz stimulation could imply that at this frequency, additional conformational changes in the proteins involved make PLA less efficient. Some modification of Cav1.1 or Panx1 affecting antibody recognition cannot be excluded at this point. In any case, this should be matter of further studies; the probably dynamic nature of Panx1–Cav1.1 interaction makes the use of real-time studies (as FRET) advisable.

It has been described that pannexin channels have themselves some voltage dependency (Iglesias and Spray, 2012) and at this stage we cannot rule out direct effects of membrane potential over pannexin channels; it appears unlikely, though, that this could be the single mechanism responsible for ATP release. More likely, the possibility of a cooperative effect between the two molecules, Cav1.1 and Panx1, should be considered albeit a detailed knowledge of pannexin channel properties is lacking.

In this work, we have observed that there were, at least, two peaks of ATP release as well as two peaks in Ins(1,4,5)P_3 production. This result is coherent with Ins(1,4,5)P_3 production occurring in response to extracellular ATP release, as reinforced by the fact that external addition of ATP induced an increase in Ins(1,4,5)P_3 levels. The mechanism for the generation of the second ATP peak is unknown; we can only speculate on the possibility that Ca^{2+} release by Ins(1,4,5)P_3R following Ins(1,4,5)P_3 production might induce the opening of pannexin channels (Locovei et al., 2006) to induce the second peak, but further experiments are needed to elucidate this point.

In conclusion, this is the first report to describe molecular events displaying frequency dependency in skeletal muscle fibers. These findings make a critical advance to our current understanding of the mechanisms by which muscle cells decipher different patterns of stimulation that underlie muscle plasticity. A new role for Cav1.1 in this frequency decoding process appears to emerge.

Materials and Methods

Isolation of adult fibers

5- to 7-week-old mice were used throughout this work. All protocols were approved by the Bioethics Committee, Faculty of Medicine, Universidad de Chile. Isolated fibers from the flexor digitorum brevis (FDB) muscle were obtained by enzymatic digestion with collagenase type II (90 min with 400 U/ml; Worthington Biochemicals Corp., Lakewood, NJ, USA), and mechanic dissociation with fire-polished Pasteur pipettes, as described previously (Casas et al., 2010). Isolated fibers were seeded in Matrigel-coated dishes and used 20 h after seeding.

Electrical stimulation

Isolated muscle fibers seeded in a dish were stimulated with 270 squared pulses of 0.3 ms duration at different frequencies with a stimulation device that consists of a row of six platinum wires intercalated 0.5 cm apart with alternate polarity across a circular plastic holder that fits in the dish. The number of pulses was kept constant at 270 pulses at every frequency tested.

Cell culture

Wild-type (wt) and dysgenic (*mdg*) primary myoblasts were cultured and differentiated for 3–4 days in DMEM low glucose 4% horse serum as described previously (Casas et al., 2012).

Reagents

Nifedipine, S(-)BayK 8644 and carbenoxolone were from Sigma. 25 μM *N*-benzyl-*p*-toluene sulphonamide (BTS, from Sigma-Aldrich Co., St Louis, MO, USA) was used in all experiments (except in calcium current measurements) as a fiber contraction inhibitor. All other reagents used were of analytical quality.

Ins(1,4,5)P_3 production measurement

Fibers were quickly frozen in liquid nitrogen at different times after stimulation and were homogenized in 20 mM Tris-HCl pH 7.5; 2 mM EDTA; 150 mM NaCl; 0.5% Triton X-100. Ins(1,4,5)P_3 production determinations were performed with a Mouse Ins(1,4,5)P_3 ELISA Kit (Cusabio Biotech, Wuhan, P.R. China) following manufacturer's instructions. The data were reported as pg of Ins(1,4,5)P_3/mg of total protein. At difference of ATP measurements, normalization by total RNA was not possible due to lysis buffer used for Ins(1,4,5)P_3 determination which is not compatible with RNA extraction.

Extracellular ATP measurement

50 μl of extracellular media aliquots from electrically stimulated or control fibers were removed at different times post-stimulation. ATP concentrations were measured with the CellTiter-Glo® Luminescent Cell Viability Assay (Promega, Madison, WI, USA), as reported (Buvinic et al., 2009). Data were calculated as pmol extracellular ATP/μg total RNA and the ratios between experimental versus control points were reported. Normalization by total RNA instead of total protein was chosen because adult muscle fibers were seeded on a Matrigel-coated surface (containing a large amount of protein), which may affect the protein determination associated to fibers only.

Measurements of the calcium current

Experiments were performed on single skeletal fibers isolated from FDB muscles of adult mice, as previously described (Jacquemond, 1997; Collet et al., 2004; Pouvreau et al., 2007). The major part of a single fiber was electrically insulated

with silicone grease so that whole-cell voltage-clamp could be achieved on a short portion of the fiber extremity. An RK-400 patch-clamp amplifier (Bio-logic, Claix, France) was used in whole-cell configuration. Command voltage pulse generation and data acquisition were done using WinWCP software (freely provided by Dr Dempster, University of Strathclyde, Glasgow, Scotland) driving an A/D, D/A converter (National Instruments, Austin, TX). Voltage-clamp was performed with a microelectrode of 1-3 MΩ resistance, filled with a solution containing (in mM): 140 potassium glutamate, 5 Na_2-ATP, 5 sodium phosphocreatine, 5.5 $MgCl_2$, 5 D-glucose, 0.1 EGTA-AM, 5 HEPES, adjusted to pH 7.2 with KOH. The extracellular solution contained (in mM): 140 tetraethylammonium-methanesulphonate, 2.5 $CaCl_2$, 2 $MgCl_2$, 0.002 tetrodotoxin,1,4-aminopyridine, 10 HEPES, adjusted to pH 7.2. The tip of the microelectrode was inserted through the silicone, within the insulated part of the fiber. Analog compensation was systematically used to decrease the effective series resistance. The Ca^{2+} current through the DHPR was recorded in response to 0.5 s-long depolarizing steps of increasing amplitude (5 mV increments), applied every 30 s from a holding potential of −80 mV. The linear leak component of the current was removed by subtracting the adequately scaled value of the steady current measured during a 20 mV hyperpolarizing step applied before each test pulse. All experiments were performed at room temperature (20–22℃).

Real-time PCR

Total RNA was obtained from skeletal muscle fibers employing Trizol reagent (Invitrogen, Corp., Carlsbad, CA, USA) according to manufacturer's protocol. cDNA was prepared from 1 µg of RNA, using SuperScript II enzyme (Invitrogen), according to manufacturer's protocol. Real-time PCR was performed using Stratagene Mx3000P (Stratagene, La Jolla, CA, USA) using the Brilliant III Ultra-Fast QPCR and QRT-PCR Master Mix amplification kit (Agilent Technologies, Santa Clara, CA, USA).

The primers used were: TnIs: 5′-GAGGTTGTGGGCTTGCTGTATGA-3′ (sense), 5′-GGAGCGCATATTAGGGATGT-3′ (antisense); TnIf: 5′-AGGT-GAAGGTGCAGAAGAGC-3′ (sense), 5′-TTGCCCCTCAGGTCAAATAG-3′ (antisense); β-actin: 5′-TCTACAATGAGCTGCGTGTG-3′ (sense), 5′-TACATG-GCTGGGGTGTTGAA-3′ (antisense). All primers used presented optimal amplification efficiency (between 90% and 110%). PCR amplification of the housekeeping gene β-actin was performed as a control. Thermocycling conditions were as follow: 95℃ for 3 min and 40 cycles of 95℃ for 10 s, 60℃ for 20 s. Expression values were normalized to β-actin and are reported in units of $2^{-\Delta\Delta CT}\pm$ s.d. as described (Pfaffl, 2001). CT value was determined by MXPro software when fluorescence was 25% higher than background. PCR products were verified by melting-curve analysis.

Immunofluorescence

Fibers were rinsed with ice-cold PBS and fixed for 20 min with paraformaldehyde (Electron Microscopy Science, Hatfield, PA, USA) 3% in PBS. Cells were rinsed with ice-cold PBS and incubated with glycine 100 mM in PBS for 10 min. Then, fibers were permeabilized with triton X-100 0.1% in PBS and blocked with 4% (w/v) BSA. Fibers were incubated with a rabbit polyclonal anti-Panx1 antibody (1:100) (designed by the group of Dr Juan Carlos Saez and directed to the non-conserved region of the C terminus of human, mouse and rat Panx1 (amino acid residues CNLGMIKMD) (Cea et al., 2012), monoclonal anti-α-actinin antibody (1:200) (Sigma-Aldrich) or monoclonal anti-Cav1.1 α1s antibody (1:100) (Thermo Scientific, Waltham, MA, USA) over night at 4℃. Finally, the cells were washed three times with PBS for 5 min each, and incubated with anti-mouse and anti-rabbit Alexa Fluor 488/Alexa Fluor 546 as appropriate. The samples were mounted in Dako anti-fading reactive (Dako, Denmark) and store at 4℃ until use.

Protein proximity studies

Cav1.1/Panx-1 interaction was detected *in situ* using the Duolink II red starter kit (Olink Bioscience, Uppsala, Sweden) according to manufacturer instructions. Briefly, primary antibodies against α1s subunit of Cav1.1 and Panx1 were applied over night at 4℃ in a humid chamber. Duolink plus and minus secondary antibodies against the primary antibodies were then incubated for 1 h at 37℃. These secondary antibodies were provided as conjugates to oligonucleotides that were tied together in a closed circle by Duolink Ligation Solution, if the antibodies were in close proximity (<40 nm). Finally, polymerase was added, to amplify any existing closed circles, and detection was achieved with complementary fluorescently labeled oligonucleotides. To define fiber structure, after PLA probes an immunofluorescence against RyR1 was performed. As negative control we performed a PLA between two proteins known for do not interact, as α-Actinin and SERCA1.

Image acquisition and processing

All images were acquired with a Carl Zeiss Axiovert 135 M Laser Scanning Microscope, with an Apo Plan 63×, NA 1.4 objective. Images deconvolution and processing were performed using ImageJ software (NIH).

Isolation of skeletal triads or T-tubules

Preparation of triad-enriched fractions from back and limbs muscles derived from 6- to 8-week-old BalbC mice were performed as previously standardized in our laboratory for frog and rabbit muscles, using differential centrifugation (Hidalgo et al., 1986; Jaimovich et al., 1986; Hidalgo et al., 2006).

Co-immunoprecipitation assay and immunoblot

Triad-enriched fractions (100 µg of protein) were solubilized for 1 h in 200 µl of lysis buffer (20 mM Tris-HCl pH 7.4, 0.1% Nonidet P-40, 5 mM EDTA pH 8, 10 mM EGTA pH 7.8, 140 mM NaCl, 10% glycerol and protease inhibitors). A 20 min, 15,000 ***g*** supernatant fraction was incubated 30 min with 10 µg A/G agarose as a pre-clearing strategy. The beads were spun down by centrifugation and washed 3 times with 200 µl of washing buffer (25 mM HEPES pH 7.5, 0.2% Nonidet P-40, 140 mM NaCl, 0.1% BSA, 10% glycerol and protease inhibitors). After the pre-clearing step, the whole cell extracts were incubated for 4 h with the correspondent antibody and then incubated 30 min with 50 µg A/G agarose beads. The beads pellet was washed three times with washing buffer. The whole amount of protein obtained after this step was resolved by SDS-PAGE in 7–10% gels, transferred to polyvinylidene difluoride filters and blotted with the corresponding antibody. To evaluate the protein content in the input of triads (prior to immunoprecipitation), 10–15 µg of protein form triads were loaded in each lane.

Data analysis

Results of n experiments are expressed as means ± s.e.m. The significance of differences was evaluated using Student's t-test for paired data and one-way ANOVA followed by Dunnett's post-test for multiple comparisons or Bonferroni's post-test for multiple paired comparisons. A $P<0.05$ was considered to be statistically significant.

Acknowledgements

We thank Dr Jordi Molgo for the gift of Xestospongin B, Dr José Miguel Eltit for help in the preparation of this manuscript and Dr Cecilia Hidalgo for valuable comments in reviewing this manuscript.

Author contributions

M.C., E.J., S.B. and V.J. designed methods and experiments; G.J., F.A., A.C.F., G.A., V.J. and M.C. performed the experiments; G.J., M.C., A.C.F., S.B. and V.J. analyzed the data; M.C., G.J., S.B., E.J., V.J. interpreted the results; and M.C. wrote the paper.

Funding

This work was supported by Fondo Nacional de Desarrollo Científico y Tecnológico [grant numbers 1110467 to E.J., M.C. and S.B.-11100454 to S.B., 3110170 to A.C.F.]; Comisión Nacional de Investigación Científica y Tecnológica [grants ACT-1111 to E.J., M.C. and S.B., AT 24110054 to G.J., AT 24100066 to F.A., 79090021 to S.B.]; Programa de Cooperación Científica Internacional Comisión Nacional de Investigación Científica y Tecnológica – Centre National de la Recherche Scientifique (CONICYT-CNRS EDC24748) to E.J., V.J. and M.C.; Program U-INICIA VID 2011, grant UINICIA 02/12M, and the University of Chile to M.C.

Supplementary material available online at
http://jcs.biologists.org/lookup/suppl/doi:10.1242/jcs.116855/-/DC1

References

Banerjee-Basu, S. and Buonanno, A. (1993). cis-acting sequences of the rat troponin I slow gene confer tissue- and development-specific transcription in cultured muscle cells as well as fiber type specificity in transgenic mice. *Mol. Cell. Biol.* **13**, 7019-7028.

Baranova, A., Ivanov, D., Petrash, N., Pestova, A., Skoblov, M., Kelmanson, I., Shagin, D., Nazarenko, S., Geraymovych, E., Litvin, O. et al. (2004). The mammalian pannexin family is homologous to the invertebrate innexin gap junction proteins. *Genomics* **83**, 706-716.

Beam, K. G. and Bannister, R. A. (2010). Looking for answers to EC coupling's persistent questions. *J. Gen. Physiol.* **136**, 7-12.

Blaauw, B., Del Piccolo, P., Rodriguez, L., Hernandez Gonzalez, V. H., Agatea, L., Solagna, F., Mammano, F., Pozzan, T. and Schiaffino, S. (2012). No evidence for inositol 1,4,5-trisphosphate-dependent Ca2+ release in isolated fibers of adult mouse skeletal muscle. *J. Gen. Physiol.* **140**, 235-241.

Bruzzone, R., Barbe, M. T., Jakob, N. J. and Monyer, H. (2005). Pharmacological properties of homomeric and heteromeric pannexin hemichannels expressed in Xenopus oocytes. *J. Neurochem.* **92**, 1033-1043.

Buller, A. J., Eccles, J. C. and Eccles, R. M. (1960). Differentiation of fast and slow muscles in the cat hind limb. *J. Physiol.* **150**, 399-416.

Buvinic, S., Almarza, G., Bustamante, M., Casas, M., López, J., Riquelme, M., Sáez, J. C., Huidobro-Toro, J. P. and Jaimovich, E. (2009). ATP released by electrical stimuli elicits calcium transients and gene expression in skeletal muscle. *J. Biol. Chem.* **284**, 34490-34505.

Calvo, S., Stauffer, J., Nakayama, M. and Buonanno, A. (1996). Transcriptional control of muscle plasticity: differential regulation of troponin I genes by electrical activity. *Dev. Genet.* **19**, 169-181.

Cárdenas, C., Liberona, J. L., Molgó, J., Colasante, C., Mignery, G. A. and Jaimovich, E. (2005). Nuclear inositol 1,4,5-trisphosphate receptors regulate local Ca2+ transients and modulate cAMP response element binding protein phosphorylation. *J. Cell Sci.* **118**, 3131-3140.

Carrasco, M. A., Riveros, N., Ríos, J., Müller, M., Torres, F., Pineda, J., Lantadilla, S. and Jaimovich, E. (2003). Depolarization-induced slow calcium transients activate early genes in skeletal muscle cells. *Am. J. Physiol. Cell Physiol.* **284**, C1438-C1447.

Casas, M., Figueroa, R., Jorquera, G., Escobar, M., Molgó, J. and Jaimovich, E. (2010). IP(3)-dependent, post-tetanic calcium transients induced by electrostimulation of adult skeletal muscle fibers. *J. Gen. Physiol.* **136**, 455-467.

Casas, M., Altamirano, F. and Jaimovich, E. (2012). Measurement of calcium release due to inositol trisphosphate receptors in skeletal muscle. *Methods Mol. Biol.* **798**, 383-393.

Cea, L. A., Riquelme, M. A., Cisterna, B. A., Puebla, C., Vega, J. L., Rovegno, M. and Sáez, J. C. (2012). Connexin- and pannexin-based channels in normal skeletal muscles and their possible role in muscle atrophy. *J. Membr. Biol.* **245**, 423-436.

Chin, E. R. (2004). The role of calcium and calcium/calmodulin-dependent kinases in skeletal muscle plasticity and mitochondrial biogenesis. *Proc. Nutr. Soc.* **63**, 279-286.

Chin, E. R., Olson, E. N., Richardson, J. A., Yang, Q., Humphries, C., Shelton, J. M., Wu, H., Zhu, W., Bassel-Duby, R. and Williams, R. S. (1998). A calcineurin-dependent transcriptional pathway controls skeletal muscle fiber type. *Genes Dev.* **12**, 2499-2509.

Chin, E. R., Grange, R. W., Viau, F., Simard, A. R., Humphries, C., Shelton, J., Bassel-Duby, R., Williams, R. S. and Michel, R. N. (2003). Alterations in slow-twitch muscle phenotype in transgenic mice overexpressing the Ca2+ buffering protein parvalbumin. *J. Physiol.* **547**, 649-663.

Collet, C., Pouvreau, S., Csernoch, L., Allard, B. and Jacquemond, V. (2004). Calcium signaling in isolated skeletal muscle fibers investigated under "Silicone Voltage-Clamp" conditions. *Cell Biochem. Biophys.* **40**, 225-236.

Corriden, R. and Insel, P. A. (2010). Basal release of ATP: an autocrine-paracrine mechanism for cell regulation. *Sci. Signal.* **3**, re1.

D'hondt, C., Ponsaerts, R., De Smedt, H., Vinken, M., De Vuyst, E., De Bock, M., Wang, N., Rogiers, V., Leybaert, L., Himpens, B. et al. (2011). Pannexin channels in ATP release and beyond: an unexpected rendezvous at the endoplasmic reticulum. *Cell. Signal.* **23**, 305-316.

Delbono, O. and Meissner, G. (1996). Sarcoplasmic reticulum Ca2+ release in rat slow- and fast-twitch muscles. *J. Membr. Biol.* **151**, 123-130.

DiMario, J. X. and Stockdale, F. E. (1997). Both myoblast lineage and innervation determine fiber type and are required for expression of the slow myosin heavy chain 2 gene. *Dev. Biol.* **188**, 167-180.

Eisner, V., Parra, V., Lavandero, S., Hidalgo, C. and Jaimovich, E. (2010). Mitochondria fine-tune the slow Ca(2+) transients induced by electrical stimulation of skeletal myotubes. *Cell Calcium* **48**, 358-370.

Eltit, J. M., García, A. A., Hidalgo, J., Liberona, J. L., Chiong, M., Lavandero, S., Maldonado, E. and Jaimovich, E. (2006). Membrane electrical activity elicits inositol 1,4,5-trisphosphate-dependent slow Ca2+ signals through a Gbetagamma/phosphatidylinositol 3-kinase gamma pathway in skeletal myotubes. *J. Biol. Chem.* **281**, 12143-12154.

Galés, C., Van Durm, J. J., Schaak, S., Pontier, S., Percherancier, Y., Audet, M., Paris, H. and Bouvier, M. (2006). Probing the activation-promoted structural rearrangements in preassembled receptor-G protein complexes. *Nat. Struct. Mol. Biol.* **13**, 778-786.

Gunning, P. and Hardeman, E. (1991). Multiple mechanisms regulate muscle fiber diversity. *FASEB J.* **5**, 3064-3070.

Halls, M. L. and Cooper, D. M. (2010). Sub-picomolar relaxin signalling by a pre-assembled RXFP1, AKAP79, AC2, beta-arrestin 2, PDE4D3 complex. *EMBO J.* **29**, 2772-2787.

Harris, K. D., Hirase, H., Leinekugel, X., Henze, D. A. and Buzsáki, G. (2001). Temporal interaction between single spikes and complex spike bursts in hippocampal pyramidal cells. *Neuron* **32**, 141-149.

Hidalgo, C., González, M. E. and García, A. M. (1986). Calcium transport in transverse tubules isolated from rabbit skeletal muscle. *Biochim. Biophys. Acta* **854**, 279-286.

Hidalgo, C., Sánchez, G., Barrientos, G. and Aracena-Parks, P. (2006). A transverse tubule NADPH oxidase activity stimulates calcium release from isolated triads via ryanodine receptor type 1 S -glutathionylation. *J. Biol. Chem.* **281**, 26473-26482.

Huang, Y. J., Maruyama, Y., Dvoryanchikov, G., Pereira, E., Chaudhari, N. and Roper, S. D. (2007). The role of pannexin 1 hemichannels in ATP release and cell-cell communication in mouse taste buds. *Proc. Natl. Acad. Sci. USA* **104**, 6436-6441.

Hughes, S. M. (1998). Muscle development: electrical control of gene expression. *Curr. Biol.* **8**, R892-R894.

Iglesias, R. M. and Spray, D. C. (2012). Pannexin1-mediated ATP release provides signal transmission between Neuro2A cells. *Neurochem. Res.* **37**, 1355-1363.

Jacquemond, V. (1997). Indo-1 fluorescence signals elicited by membrane depolarization in enzymatically isolated mouse skeletal muscle fibers. *Biophys. J.* **73**, 920-928.

Jaimovich, E., Donoso, P., Liberona, J. L. and Hidalgo, C. (1986). Ion pathways in transverse tubules. Quantification of receptors in membranes isolated from frog and rabbit skeletal muscle. *Biochim. Biophys. Acta* **855**, 89-98.

Jaimovich, E., Reyes, R., Liberona, J. L. and Powell, J. A. (2000). IP(3) receptors, IP(3) transients, and nucleus-associated Ca(2+) signals in cultured skeletal muscle. *Am. J. Physiol. Cell Physiol.* **278**, C998-C1010.

Johnson, B. D., Brousal, J. P., Peterson, B. Z., Gallombardo, P. A., Hockerman, G. H., Lai, Y., Scheuer, T. and Catterall, W. A. (1997). Modulation of the cloned skeletal muscle L-type Ca2+ channel by anchored cAMP-dependent protein kinase. *J. Neurosci.* **17**, 1243-1255.

Juretić, N., Urzúa, U., Munroe, D. J., Jaimovich, E. and Riveros, N. (2007). Differential gene expression in skeletal muscle cells after membrane depolarization. *J. Cell. Physiol.* **210**, 819-830.

Kalhovde, J. M., Jerkovic, R., Sefland, I., Cordonnier, C., Calabria, E., Schiaffino, S. and Lømo, T. (2005). "Fast" and "slow" muscle fibres in hindlimb muscles of adult rats regenerate from intrinsically different satellite cells. *J. Physiol.* **562**, 847-857.

Kubis, H. P., Scheibe, R. J., Meissner, J. D., Hornung, G. and Gros, G. (2002). Fast-to-slow transformation and nuclear import/export kinetics of the transcription factor NFATc1 during electrostimulation of rabbit muscle cells in culture. *J. Physiol.* **541**, 835-847.

Lamb, G. D. (1992). DHP receptors and excitation-contraction coupling. *J. Muscle Res. Cell Motil.* **13**, 394-405.

Lamb, G. D. and Walsh, T. (1987). Calcium currents, charge movement and dihydropyridine binding in fast- and slow-twitch muscles of rat and rabbit. *J. Physiol.* **393**, 595-617.

Liu, Y., Cseresnyés, Z., Randall, W. R. and Schneider, M. F. (2001). Activity-dependent nuclear translocation and intranuclear distribution of NFATc in adult skeletal muscle fibers. *J. Cell Biol.* **155**, 27-39.

Locovei, S., Wang, J. and Dahl, G. (2006). Activation of pannexin 1 channels by ATP through P2Y receptors and by cytoplasmic calcium. *FEBS Lett.* **580**, 239-244.

Mayr, G. W. and Thieleczek, R. (1991). Masses of inositol phosphates in resting and tetanically stimulated vertebrate skeletal muscles. *Biochem. J.* **280**, 631-640.

Murgia, M., Serrano, A. L., Calabria, E., Pallafacchina, G., Lomo, T. and Schiaffino, S. (2000). Ras is involved in nerve-activity-dependent regulation of muscle genes. *Nat. Cell Biol.* **2**, 142-147.

Pette, D. and Vrbová, G. (1985). Neural control of phenotypic expression in mammalian muscle fibers. *Muscle Nerve* **8**, 676-689.

Pfaffl, M. W. (2001). A new mathematical model for relative quantification in real-time RT-PCR. *Nucleic Acids Res.* **29**, e45.

Pouvreau, S., Collet, C., Allard, B. and Jacquemond, V. (2007). Whole-cell voltage clamp on skeletal muscle fibers with the silicone-clamp technique. *Methods Mol. Biol.* **403**, 185-194.

Rana, Z. A., Gundersen, K. and Buonanno, A. (2009). The ups and downs of gene regulation by electrical activity in skeletal muscles. *J. Muscle Res. Cell Motil.* **30**, 255-260.

Ríos, E. and Pizarro, G. (1991). Voltage sensor of excitation-contraction coupling in skeletal muscle. *Physiol. Rev.* **71**, 849-908.

Rojas, C. and Jaimovich, E. (1990). Calcium release modulated by inositol trisphosphate in ruptured fibers from frog skeletal muscle. *Pflugers Arch.* **416**, 296-304.

Schiaffino, S., Murgia, M., Serrano, A. L., Calabria, E. and Pallafacchina, G. (1999). How is muscle phenotype controlled by nerve activity? *Ital. J. Neurol. Sci.* **20**, 409-412.

Schiaffino, S., Sandri, M. and Murgia, M. (2007). Activity-dependent signaling pathways controlling muscle diversity and plasticity. *Physiology (Bethesda)* **22**, 269-278.

Serrano, A. L., Murgia, M., Pallafacchina, G., Calabria, E., Coniglio, P., Lømo, T. and Schiaffino, S. (2001). Calcineurin controls nerve activity-dependent specification of slow skeletal muscle fibers but not muscle growth. *Proc. Natl. Acad. Sci. USA* **98**, 13108-13113.

Spangenburg, E. E. and Booth, F. W. (2003). Molecular regulation of individual skeletal muscle fibre types. *Acta Physiol. Scand.* **178**, 413-424.

Vergara, J., Tsien, R. Y. and Delay, M. (1985). Inositol 1,4,5-trisphosphate: a possible chemical link in excitation-contraction coupling in muscle. *Proc. Natl. Acad. Sci. USA* **82**, 6352-6356.

Volpe, P., Salviati, G., Di Virgilio, F. and Pozzan, T. (1985). Inositol 1,4,5-trisphosphate induces calcium release from sarcoplasmic reticulum of skeletal muscle. *Nature* **316**, 347-349.

Wheeler, D. G., Groth, R. D., Ma, H., Barrett, C. F., Owen, S. F., Safa, P. and Tsien, R. W. (2012). Ca(V)1 and Ca(V)2 channels engage distinct modes of Ca(2+) signaling to control CREB-dependent gene expression. *Cell* **149**, 1112-1124.

Wu, H., Kanatous, S. B., Thurmond, F. A., Gallardo, T., Isotani, E., Bassel-Duby, R. and Williams, R. S. (2002). Regulation of mitochondrial biogenesis in skeletal muscle by CaMK. *Science* **296**, 349-352.

Xu, W., Morishita, W., Buckmaster, P. S., Pang, Z. P., Malenka, R. C. and Südhof, T. C. (2012). Distinct neuronal coding schemes in memory revealed by selective erasure of fast synchronous synaptic transmission. *Neuron* **73**, 990-1001.